Review of Diagnostics for Next Generation Linear Accelerators

M. Ross

REVIEW OF DIAGNOSTICS FOR NEXT GENERATION LINEAR ACCELERATORS

M. Ross, Stanford Linear Accelerator Center, Stanford, CA 94309, USA

Abstract

New electron linac designs incorporate substantial advances in critical beam parameters such as beam loading and bunch length and will require new levels of performance in stability and phase space control. In the coming decade, e- (and e+) linacs will be built for a high power linear collider (TESLA, CLIC, JLC/NLC), for fourth generation X-ray sources (TESLA FEL, LCLS, Spring 8 FEL) and for basic accelerator research and development (Orion). Each project assumes significant instrumentation performance advances across a wide front.

This review will focus on basic diagnostics for beam position and phase space monitoring. Research and development efforts aimed at high precision multi-bunch beam position monitors, transverse and longitudinal profile monitors and timing systems will be described.

1 INTRODUCTION

Next generation linacs have smaller beam sizes, increased stability and improved acceleration efficiency. They will be used for single pass free electron lasers (FEL) [1], linear colliders (LC) [2] and advanced accelerator research and development [3]. Table 1 shows the evolution of beam parameters from the SLAC Linear Collider (SLC) toward the next generation projects. Performance improvements of a factor 10 are typical. If we consider older, more conventional linacs, the relative changes in performance parameters are more impressive, often as much as a factor of 1000. In addition, there are special locations within the linac system where the beam requirements are much more stringent: for example at the LC interaction point or within the FEL undulator.

Table 1: Next generation linac parameter comparison for SLC (1985), the SLAC Linac Coherent Light Source (LCLS) and the Next Linear Collider (NLC).

	SLC	LCLS	NLC
σ x (μm)	90	30	7
σ y (μm)	50	30	1
σ z (μm)	1300	30	100
peak I (A)	700	3400	1000
power density (W/m^2)	2e13	1e12	1e18

It is evident that new technology and different physical principles, such as diffraction radiation and Compton scattering, are needed in order to extend the performance of diagnostics to meet the challenge [4]. In this paper we will review ideas and tests of diagnostics for measuring electron beam position, profile (transverse and longitudinal) and loss.

2 POSITION

2.1 Purposes

High peak current linacs require accurate, well referenced, beam position monitors (BPM's) to suppress the interaction between the RF structure and the beam. In addition, equally as important, the small beam must pass close to the center of each quadrupole magnet in order to avoid emittance dilution arising from the dispersion generated from a small dipole kick. Some LC designs include two separate BPM systems in each linac. Typical requirements are shown in table 2.

Table 2: NLC Linac quadrupole BPM performance requirements

Parameter	Value	Conditions
Resolution	300 nm rms	@ 10^{10} e- single bunch
Position Stability	1 μm	over 24 hours
Position Accuracy	200 μm	wrt the quad magnetic center
x,y dynamic range	± 2 mm	
Q dynamic range (per bunch)	5×10^8 to 1.5×10^{10} e-	

The most challenging requirement is the long-term position stability, $\sim 2 \times 10^{-4}$ r_0 (r_0=BPM radius). The planned resolution is $\sim 6 \times 10^{-5}$ r_0; both are a factor of 50 improvement over BPMs used in the SLC.

The BPM's are in continual use by an automated steering loop that keeps the beam centered in the accelerating structure and the quadrupole magnets. The model for operation of the linac assumes that a second, presumably more intrusive, automatic quadrupole beam centering procedure is implemented once per day, as required by long term BPM drifts.

BPM system requirements for the FEL are tightest in the undulator itself. For full coherent emission saturation, the beam and the light it has generated must remain superimposed throughout the undulator. Surprisingly, longitudinal considerations rather than transverse set the steering tolerances. The difference between the xray

photon path length and the electron beam must remain less than a full x-ray wavelength (0.1 nm for LCLS) integrated over the full undulator length. Beam-based alignment is used to correct the trajectory in the absolute sense, so that it is as straight as the optical path. For LCLS, the proposed beam based alignment scheme uses trajectory data taken at very different energies, down to 1/3 of the nominal energy. Transverse overlap, also important, requires beam-x ray profile monitors and x-ray flux monitors [5].

2.2 Designs

Table 1 shows the beam power density increase between SLC, the prototype linear collider, and NLC. Roughly half of the increase is from raising the number of bunches accelerated on each linac pulse from 1 to ~100. The BPM system must be able to resolve the position of single bunches (or groups of bunches) spaced at 2.8 ns. A proposed design for a multi-bunch BPM [6] uses a heterodyne receiver, tuned near the peak response frequency of the pickup buttons, followed by broadband digitizer electronics. Calibration is done using both a local oscillator tone generator and the single bunch impulse response. Design challenges include deconvolving the multi-bunch signal and reducing the cost of the broadband digitiser.

3 TRANSVERSE PROFILE

3.1 Operational considerations

For both an LC and an FEL, the beam size is a critical operational parameter. The luminosity L of an LC is:

$$L = \frac{P_B}{E_{CM}} \times \frac{N_e}{4\pi\sigma_x^* \sigma_y^*} \times H_D$$

where P_b is the beam power, E_{cm} is the center of mass energy, N_e is the number of particles in a single bunch, $\sigma_{x,y}^*$ is the beam size at the interaction point and H_D is the enhancement from the inter-bunch focusing effect. In practice, once the machine is built, the beam size is controlled more effectively than the other parameters. Since there is no transverse equilibrium condition in a linac, $\sigma_{x,y}^*$ is determined by the beam source and the sum (or product) of dilutions in the acceleration and delivery system. The primary function of the transverse profile monitor is as a predictor of luminosity. Second, if implemented in groups along the linac length, they can be used to determine sources of emittance dilution.

Profile monitors fall into two categories: 1) particle density samplers (e.g wire scanners) and 2) optical devices (imagers of phosphorescence, transition radiation or synchrotron radiation). In the next section we will examine examples of each of these.

A predictor of luminosity, the absolute measurement produced by the monitor is extremely important.

However, given the sparse distribution of profile monitors it is difficult to verify their performance. In contrast, the ubiquitous BPM's can be used to check each other and can be compared with the expected beam motion from magnetic field changes. Techniques for verifying profile monitor performance include 1) redundancy, 2) using the centroid motion as a BPM, 3) combining monitors of different technologies and 4) use of flexible beam optics for producing a variety of beam conditions.

A good example of the implementation of these checks can be seen at the Accelerator Test Facility at KEK (ATF) [7, 8]. The primary purpose of the ATF is to test the generation of beams for an LC. As such, it produces 1.3 GeV, 20 bunch, damped electron beams with emittance $\varepsilon_{x,y} = 2 \times 0.02$ nm (1 nC), some of the smallest beams ever produced. The ATF beam is extracted from its damping ring and delivered to a transport that includes a diagnostic system. A sequence of five wire scanners is used for measuring $\varepsilon_{x,y}$.

In principle, only three independent measurements of beam size are required to determine the volume of beam phase space in a given direction ($\sigma_x, \sigma_{x'}$) and its correlation($\sigma_{xx'}$). Each measurement must be done with a different rotation of beam phase space. Typically the rotation is naturally given by the spacing of a group of monitors or is directly implemented for a single monitor by changing upstream focus magnets. In practice, the quantity

$$\beta_{mag}\varepsilon = \frac{1}{2}\left[\beta\tilde{\gamma} - 2\alpha\tilde{\alpha} + \gamma\tilde{\beta}\right]\varepsilon,$$

where β_{mag} is an indicator of beam to lattice mismatch and the '~' indicates the measured optical functions, is both a more useful approximation of the eventual beam size following filamentation in the linac and a more accurately and simply measured quantity[9]. For a perfectly beta-matched beam, $\beta_{mag} = 1$.

The fully filamented emittance, $\beta_{mag}\varepsilon$, can be estimated from the measured beam size matrix [10] and the design optics,

$$\sigma = \begin{bmatrix} \sigma_{11} & \sigma_{12} \\ \sigma_{21} & \sigma_{22} \end{bmatrix} \quad \text{and} \quad A = \frac{1}{\sqrt{\beta}}\begin{bmatrix} \beta & 0 \\ -\alpha & 1 \end{bmatrix}$$

(the phase space rotation between each of the scans must be well known) using

$$\hat{\sigma} = A^{-1}\sigma\left(A^{-1}\right)^T,$$

then $\beta_{mag}\varepsilon = \frac{1}{2}Tr(\hat{\sigma})$. In the presence of errors, the estimated emittance ($\varepsilon = \sqrt{\det(\sigma)}$) can be imaginary, but $\beta_{mag}\varepsilon$ is always positive.

Both an LC and an FEL include phase space manipulation systems for longitudinal compression. The compressor optics are usually quite complex and require high quality, tight tolerance magnets. Accurate phase

space monitors are required before and after the bunch compressor.

3.2 Designs - Laser based scanners

Laser based scanners will be required for the LC due to the very high beam power density [11], well beyond the failure threshold of any wire material. Recently, a new type of laser based scanner, built at ATF / KEK, [12] has produced results and can be added to the two types tested at SLAC [13][14]. The device, shown in figure 1, perhaps best suited for rings or CW linacs, uses a transversely mounted resonant Fabry-Perot optical resonant cavity focused so that a very fine laser waist is produced at its center. In this case, the Q of the cavity amplifies the incoming CW laser power by a factor of 300. Compton scattered photons are detected following a bending magnet.

3.3 Designs - Optical Transition Radiation Profile Monitors

Transition radiation tests of both a high resolution optical monitor [15] and diffraction or edge radiation have been done in the ATF extraction line. Figure 3 shows the 2 μm resolution optical transition radiation monitor. Backward transition radiation, emerging at the angle of specular reflection, is easiest to image since the microscope objective can be located quite close to the target. The monitor shown in figure 3 has a optical working distance of 35 mm. Tests done at ATF with a $\sigma_{x,y}$=20 μm x 12 μm, 1 nC bunch showed target surface damage after a few hundred pulses at 1 Hz. Forward radiation is collinear with the beam and presumably less affected by surface defects. Unfortunately, since a mirror is required to deflect the transition radiation away from the beam path, achieving very small working distances will be difficult.
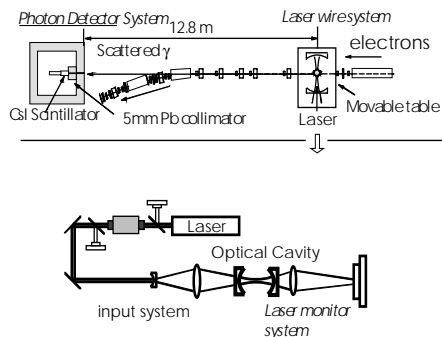

Figure 1: ATF CW laser-based profile monitor schematic.
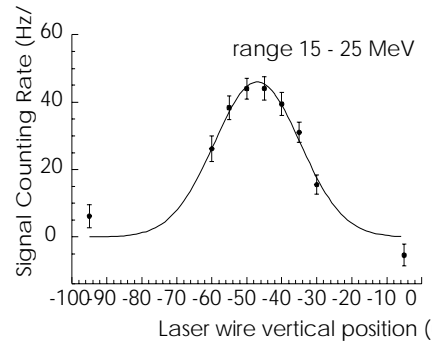

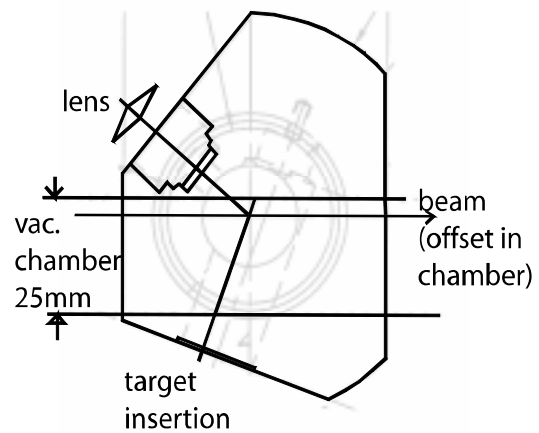Figure 2: ATF resonant optical cavity beam size scan.

Figure 3: High-resolution optical transition radiation monitor tested at ATF/KEK. The monitor is displaced when the target is inserted in order to bring the beam close to the lens.

4 LONGITUDINAL PROFILE

4.1 Challenge

Most LC and FEL designs include one or more stages of bunch length compression, where the bunch is rotated in longitudinal phase space, exchanging energy spread for bunch length. In the LCLS FEL design, each stage is followed by a linac section, which reduces the fractional energy spread. An aggressive bunch compression scheme, shown in figure 4, involves generating a strong correlation between E and z with offset phase RF and using a sequence bend magnets or chicane to provide different path lengths for the head and tail particles. The scheme relies on careful cancellation between the longitudinal beam wakefield and the slope of the S-band RF. Because the beam is far from the RF crest in the section of linac where the correlation is generated, the pulse to pulse phase stability and beam loading stability tolerances are extreme: 0.1 degrees S-band for ~ 35 klystrons and 0.2% beam intensity at 1 nC.

The z distributions shown in figure 4 illustrate the challenge of measuring the bunch length. It is clear that

the two traditional methods of bunch length monitoring, the streak camera and the inverse transform of the emitted radiation do not have the required resolution. The best streak cameras have resolution approaching 0.3 fs, ~100 μm, about 6 times the effective σ_z of LCLS.

Coherent radiation on the other hand is expected to be a significant source of emittance dilution at a short wavelength FEL. There will be ample opportunity to study this relatively new beam diagnostic tool. However, since coherent radiation monitors provide only radiated power spectrum information, without phase, they will not yield shape information for the highly asymmetric bunches with close to 10 μm detail.

4.2 Design - LCLS Bunch Length Monitor

The solution adopted for LCLS is an old idea [16] that relies on a transverse deflecting TM_{11} disk loaded waveguide structure [17]. The design parameters of the LCLS bunch length monitor are shown in Table 3 and the scheme is shown in Figure 5. The S-band TM_{11} deflecting field is used to tilt the beam, introducing a $y - z$ correlation. The phase of the deflection is offset slightly so that the centroid of the beam receives a small kick directing it onto a downstream screen. This allows operation of the monitor in 'parasitic' mode, so that only those machine pulses during which the deflection RF is on are intercepted by the screen and all other beam pulses proceed to the undulator downstream. By alternating the sign of the $y - z$ correlation, incoming correlations, such as those generated by wakefields, can be checked and corrected for.

Table 3: LCLS Bunch length monitor parameters for the SLAC S-band 8 foot TM_{11} deflecting structure.

RF deflector voltage	20 MV
Peak input power	25 MW
RF deflector phase (crest at 90°)	3.3 deg
Nominal beam size	80 μm
Beam size with deflector on (two-phase mean)	272 μm
Beam energy at deflector	5.4 GeV
RMS bunch length	24 μm

The bunch length is given by a function of the accelerator properties, the structure gradient and the screen measurements:

$$\sigma_z = \frac{\lambda_{rf}}{2\pi} \frac{\sqrt{E_d E_s}}{\left| eV_0 \sin \Delta\psi \cos\varphi \right|} \sqrt{\frac{\left(\sigma_y^2 - \sigma_{y0}^2 \right)}{\beta_d \beta_s}}$$

where λ_{rf} is the RF wavelength, $E_{d,s}$ is the beam energy at the deflector and screen, $\Delta\psi$ is the betatron phase advance between the deflector and the screen, φ is the phase offset of the RF ($\equiv$0 at the zero crossing), σ_y is the measured beam size on the screen, σ_{y0} is the beam size without the

y-z correlation and $\beta_{d,s}$ are the beta functions at the screen and deflector.
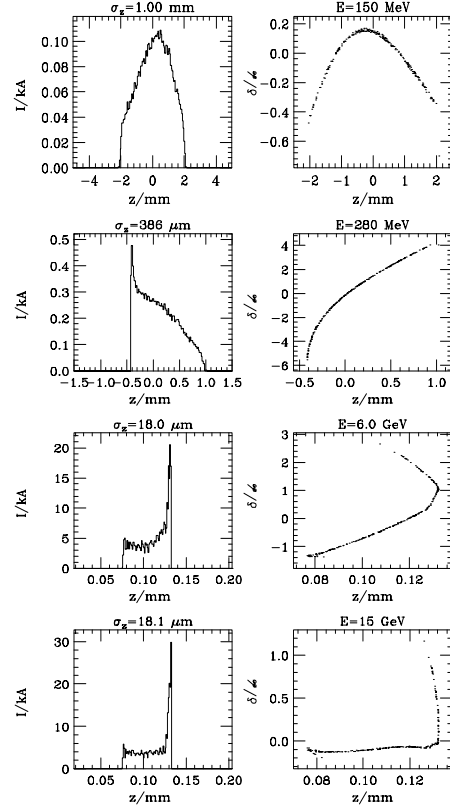

Figure 4: Evolution of longitudinal phase space in the LCLS. The plots show the z distribution and the E – z correlation following (from top to bottom): a) the gun capture section, b) the first compressor section, c) the second compressor and d) at the end of the linac.
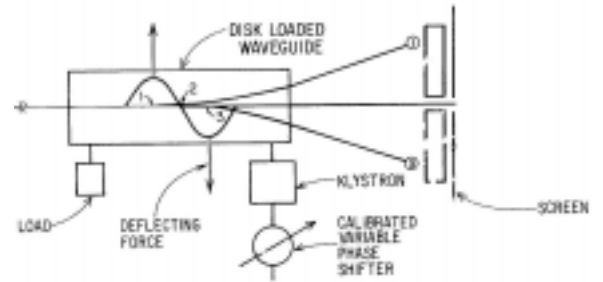

Figure 5: Schematic of bunch length monitor using RF transverse deflecting structure.

4.3 Beam phase monitoring

Both an LC and an FEL use linac structures far from the peak gradient in order to take advantage of the derivative of the gradient. Roughly 1/3 of the LCLS linac is operated 45 degrees from crest. The tolerance for phasing the bunches with respect to the RF is reduced by a factor of 10 from earlier linacs. In addition, next generation linac systems have non-isochronous systems

between accelerating structures, as at KEK [18, 19] and TJNAF.

At an LC, the timing system is coupled with a beam phase monitoring so that the timing system requirements are defined only for the production of a pilot beam. The beam phase detection system then locks onto the difference between the beam and RF phase closes the loop. The two innovative components are the timing distribution system, with a tolerance of 1 degree X-band (0.2 ps) over time scales of 1 minute throughout the 15 km typical distribution length, [20] and the beam phase system.

REFERENCES

[1] J. Arthur et.al., LINAC Coherent Light Source Design Study Report, SLAC-R-0521, 1998.

[2] A. Wagner et.al., TESLA: the Superconducting Electron Positron Linear Collider with an Integrated X-Ray Laser Laboratory, Technical Design Report, DESY, 2001. http://tesla.desy.de/new_pages/TDR_CD/start.html

[3] Proceedings of the 9th Advanced Accelerator Concepts Workshop, Santa Fe, NM, 2000 (AIP Proceedings to be published). http://www-project.slac.stanford.edu/orion/Presentations/orion%20aac.pdf

[4] M. Ross, 'Linear Collider Diagnostics', Presented at the 9th Beam Instrumentation Workshop, Cambridge MA, 2000, AIP Conference Proceedings 546, 147:163. (SLAC–PUB-8437).

[5] E. Gluskin, et.al., 'Predicted Performance of the LCLS X-Ray Diagnostics', http://www-ssrl.slac.stanford.edu/lcls/technotes/LCLS-TN-00-13.pdf

[6] S. Anderson, et.al., 'Design of a Multi-bunch BPM for the Next Linear Collider', these proceedings.

[7] H. Hayano, ' Wire Scanners for Small Emittance Beam Measurement in ATF', presented at the 20th International Linac Conference, Monterey, CA, 2000.

[8] K. Kubo, 'Recent Progress in Accelerator Test Facility at KEK', presented at the 18th International Conference on High Energy Accelerators, Tsukuba, 2001.

[9] F. Decker et.al., 'Dispersion and Betatron Matching into the Linac', presented at the IEEE 1991 Particle Accelerator Conference, San Francisco, CA, 1991. (SLAC-PUB-5484)

[10] K. Brown, et.al., 'TRANSPORT/360', SLAC-R-091, 1970.

[11] C. Field, et.al., 'Wire Breakage in SLC Wire Profile Monitors' presented at the 8th Beam Instrumentation Workshop, Stanford, CA, 1998 (SLAC-PUB-7832).

[12] H. Sakai, et.al., 'Measurement of an Electron Beam Size with a Laser Wire Beam Profile Monitor', Phys.Rev.ST Accel.Beams 4:022801,2001.

[13] M. Ross, et.al., 'A High Performance Spot Size Monitor', presented at the 18th International Linac Conference, Geneva, 1996.

[14] T. Shintake, et.al., 'Experiments of Nanometer Spot Size Monitor at FFTB using Laser Interferometry', presented at 1995 IEEE Particle Accelerator Conference, Dallas, TX, 1995.

[15] M. Ross, et.al., 'A Very High Resolution Optical Transition Radiation Beam Profile Monitor', to be presented at 2001 IEEE Particle Accelerator Conference, Chicago, IL, 2001.

[16] G. A. Loew and O. H Altenmueller, 'Design and Applications of RF Separator Structures at SLAC', presented at the 5th International Conference on High-Energy Accelerators, Frascati, 1965. and O. Altenmueller, et.al., 'Investigations of Traveling Wave Separators for the Stanford 2-Mile Accelerator', Rev.Sci.Instrum. 35:438-442,1964.

[17] P. Krejcik, et. al., 'A Transverse RF Deflecting Structure for Bunch Length and Phase Space Diagnostics', to be presented at 2001 IEEE Particle Accelerator Conference, Chicago, IL, 2001. and P. Emma, et.al., 'A Transverse RF Deflecting Structure for Bunch Length and Phase Space Diagnostics', LCLS-TN-00-12, http://www-ssrl.slac.stanford.edu/lcls/technotes/LCLS-TN-00-12.pdf .

[18] A. Enomoto, et.al., 'Construction Status of the KEK B 8-GeV Injector Linac', presented at 1st Asian Particle Accelerator Conference, Tsukuba, 1998.

[19]Y. Ogawa, et.al., 'New Streak Camera System for the KEK B Linac', presented at 1st Asian Particle Accelerator Conference, Tsukuba, Japan, 1998.

[20] J. Frisch, et.al., 'The RF Phase Distribution and Timing System for the NLC', presented at 20th International Linac Conference, Monterey, CA, 2000 (SLAC-PUB-8578).